Received: 17 April 2023 | Accepted: 6 October 2023

DOI: 10.1111/fcp.12961

ORIGINAL ARTICLE

Fundamental & Clinical Pharmacology | WILEY

Epothilone B loaded in acellular nerve allograft enhanced sciatic nerve regeneration in rats

Zhikal Omar Khudhur[1] | **Shang Ziyad Abdulqadir**[2] | **Abdullah Faqiyazdin Ahmed Mzury**[3] | **Abdulrahman Aziz Rasoul**[3] | **Shukur Wasman Smail**[2,4] | **Mohammad B. Ghayour**[5] | **Arash Abdolmaleki**[6]

[1]Department of Biology Education, Faculty of Education, Tishk International University, Erbil, Kurdistan Region, Iraq

[2]Department of Biology, College of Science, Salahaddin University-Erbil, Iraq

[3]KBMS, College of Medicine, Hawler Medical University, Erbil, Kurdistan Region, Iraq

[4]Department of Medical Microbiology, College of Science, Cihan University-Erbil, Kurdistan Region, Iraq

[5]Department of Biology, Faculty of Science, Ferdowsi University of Mashhad, Mashhad, Iran

[6]Department of Biophysics, Faculty of Advanced Technologies, University of Mohaghegh Ardabili, Namin, Iran

Correspondence
Arash Abdolmaleki, Department of Biophysics, Faculty of Advanced Technologies, University of Mohaghegh Ardabili, Namin, Iran.
Email: abdolmalekiarash1364@gmail.com; abdolmalekiarash1364@uma.ac.ir

Zhikal Omar Khudhur, Department of Biology Education, Faculty of Education, Tishk International University, Erbil, Kurdistan Region, Iraq.
Email: zhikal.omer@tiu.edu.iq

Funding information
University of Mohaghegh Ardabili, Iran; Tishk International University, Erbil, Kurdistan Region, Iraq, Grant/Award Number: 923

Abstract

Background: Epothilone B (EpoB) is a microtubule-stabilizing agent with neuroprotective properties.

Objectives: This study examines the regenerative properties of ANA supplemented with EpoB on a sciatic nerve deficit in male Wistar rats.

Methods: For this purpose, the 10 mm nerve gap was filled with acellular nerve allografts (ANAs) containing EpoB at 0.1, 1, and 10 nM concentrations. The sensorimotor recovery was evaluated up to 16 weeks after the operation. Real-time PCR, histomorphometry analysis, and electrophysiological evaluation were also used to evaluate the process of nerve regeneration.

Results: ANA/EpoB (0.1 nM) significantly improved sensorimotor recovery in rats compared to ANA, ANA/EpoB (1 nM), and ANA/EpoB (10 nM) groups. This led to reduced muscle atrophy, improved sciatic functional index, and thermal paw withdrawal reflex latency, indicating nerve regeneration and target organ reinnervation. The electrophysiological and histomorphometry findings also confirmed the ANA/EpoB regenerative properties (0.1 nM). EpoB only enhanced ANA regenerative properties at 0.1 nM, with no therapeutic effects at higher concentrations.

Conclusion: Totally, we concluded that ANA loaded with 0.1 nM EpoB can effectively reconstruct the transected sciatic nerve in rats, likely by enhancing axonal sprouting and extension.

KEYWORDS
allograft, decellularization, EpoB, regeneration, sciatic nerve

[Correction added on 6 February 2024, after first online publication: Affiliations 1 and 2 have been updated in this version.]

Abbreviations: ANAs, acellular nerve allografts; ANOVA, a one-way analysis of variance; CMAP, compound muscle action potential; EpoB, epothilone B; FDA, Food and Drug Administration; GAPDH, glyceraldehyde 3-phosphate dehydrogenase; H&E, hematoxylin–eosin; ITS, intermediary toe spread; NCV, nerve conduction velocity; PBS, phosphate-buffered sodium solution; PFA, paraformaldehyde; PL, paw length; PNI, peripheral nerve injury; PWRL, thermal paw withdrawal reflex latency; SB-10, sulfobetaine-10; SB-16, sulfobetaine-16; SCs, Schwann cells; SFI, sciatic functional index; TS, toe spread.

1 | INTRODUCTION

Peripheral nerve injury (PNI) is a common clinical problem that affects more than five million new subjects worldwide annually [1]. Despite the inherent regenerative capacity of peripheral nerves, severe lesions often result in insufficient recovery, especially in cases with large nerve gaps [2]. When a long length of nerve is destroyed and direct coaptation is not possible, nerve autografting is the standard treatment [3]. However, nerve autografts face limitations in clinical use due to donor scarcity, size mismatch, donor site morbidity, additional surgeries, and neuroma formation [4, 5]. As a result, numerous studies are underway to develop tissue-engineered scaffolds to bridge nerve stumps. The physical and biochemical architecture of fabricated scaffolds should mimic the native nerve's extracellular matrix to support axon growth and myelination [6–8].

Acellular nerve allografts (ANAs) offer a biological scaffold as a promising alternative to nerve autografts. Despite the loss of cells, ANA preserves a highly organized ECM structure that provides a supporting substrate for regenerating axons [9]. Decellularization also diminishes graft immunogenicity by removing immunogenic elements [10]. Nevertheless, the regeneration outcome of ANA is commonly inferior to nerve autograft, particularly over long lesion gaps [11]. As a result, efforts were made to improve the ANA's efficiency using growth-stimulating agents, neuroprotective factors, and cell transplantation [8, 11, 12]. In this regard, microtubule-stabilizing agents show potential for treating traumatic neural injuries and neurodegenerative disorders [13, 14]. They can speed up microtubule polymerization as the main cytoskeleton component. Microtubules play crucial roles in neuronal functions like intracellular transport, cellular polarity, cell motility, mitosis, cytokinesis, and neuronal growth [13]. They are dynamic linear tubular polymers consisting of α- and β-tubulin heterodimers, constantly assembled and disassembled by tubulin subunit addition and removal [15]. Microtubule assembly and actin filament polymerization in the growth cone enhance neurite outgrowth and axon elongation [16, 17]. The growth cone is a dynamic structure rich in microtubules and actin filaments that dynamically generates movements for axon extension or retraction in response to environmental cues [18–20]. Following Wallerian degeneration, growth cones develop at the tips of regenerating axons and grow along the bands of Bungner created by Schwann cells (SCs) [21]. Microtubule disorganization also contributes to the pathogenesis of neurodegenerative diseases such as Alzheimer's and Parkinson's.

Epothilone B (EpoB), a microtubule-stabilizing agent, induces neurite outgrowth and axon elongation in rodent models by enhancing microtubule polymerization and stabilization at the growth cone [22, 23]. This macrolide, derived from the myxobacterium *Sorangium cellulosum*, can enhance microtubule polymerization even in the lack of GTP or microtubule-associated proteins. Based on this feature, EpoB can prevent the division of malignant cells by interfering with mitotic spindle detachment from centrosomes and inhibiting the G2-M transition cell cycle phase. The US Food and Drug Administration (FDA) has approved EpoB for cancer treatment. In addition, in the rodent model of brain and spinal cord injuries, EpoB could enhance axonal regeneration. It reduces astroglial-fibrotic scars, which exacerbate axonal outgrowth following a stroke or traumatic CNS injuries [23–25]. Systemic administration of EpoB could also improve cognitive abilities by preventing axonal microtubule degeneration in a murine model of neurodegenerative tauopathies [26]. Furthermore, microtubule stabilization demonstrated neuroprotective effects in a murine model of MPTP-induced Parkinson's [27]. Zhou et al. show EpoB systemic administration improves axonal regeneration and functional recovery in rats with sciatic nerve crush. This is likely due to its ability to promote SC autophagy and migration [28]. In contrast, some studies have reported the adverse effects of this drug on neural regeneration and functional recovery. For example, Chiorazzi et al. suggested that EpoB has dose-dependent neurotoxic effects on peripheral nerves in Wistar and Fischer rats [29]. Additionally, systemic administration of EpoB as a general inhibitor of cell division is accompanied by significant side effects. Given the conflicting evidence regarding the neuroprotective effects of EpoB and the insufficiency of data on its impacts on PNI regeneration, this study aimed to investigate the regenerative properties of the ANA supplemented with EpoB on a 10 mm sciatic nerve defect in male Wistar rats.

2 | METHODS

2.1 | Animals and experimental groups

In this experiment, seventy 2- to 3-month-old male Wistar rats weighing 200 ± 20 g were used. The animals were kept in plexiglass cages in groups of three, with unlimited access to standard rodent chow and water. The experimental procedures adhered to the guidelines developed by the University of Mohaghegh Ardabili's (Ardabil, Iran) ethical committee for the care and use of laboratory animals. The rats were randomly assigned into seven groups ($n = 10$): a sham control group in which the sciatic nerve was only exposed, without any lesion or treatment; an autograft group in which the sciatic nerve gap was reconstructed by nerve autografting; an ANA group in which the nerve gap was bridged by ANA; an ANA/vehicle group in which the nerve gap was reconstructed by the ANA loaded with drug vehicle; and three ANA/EpoB treatment groups in which the nerve gaps were bridged by the ANA supplemented with EpoB at 0.1, 1, or 10 nM concentrations.

The concentrations of EpoB were chosen based on previous research [30]. Sham surgery is an intervention that omits the step thought to be therapeutically necessary. In surgical intervention, sham surgery serves an analogous purpose to placebo drugs, neutralizing biases such as the placebo effect. The sham surgery group is necessary to prove that sensory-motor deficits are directly caused by cutting the sciatic nerve, not other injuries that inevitably occur during surgery to the surrounding tissues [31]. For this purpose, to this end, the sham surgery group should be compared to the healthy controls to determine whether the surgical procedures (except nerve injury) could cause a change in the normal parameters. Sham surgery is widely used in surgical research, including studies on sciatic nerve regeneration [32–34]. Because no significant difference was observed between the sham surgery and healthy control groups, the data from the healthy groups were not shown to simplify the graphs. Furthermore, the experimental groups were compared to the autograft group because it is the gold standard for nerve grafting in the clinic (positive control group).

2.2 | ANA preparation

Sciatic nerve allografts from male Wistar rats were chemically decellularized, as previously described by Hudson et al. [35]. In brief, sciatic nerves were harvested from donors and trimmed to 15 mm under aseptic conditions. The nerve segments were then agitated in deionized distilled water at room temperature for 7 h. The specimens were then exposed for 15 h to 125 mM sulfobetaine-10 (SB-10) (Sigma) in a phosphate-buffered sodium solution (PBS). Following that, they were subjected to a 24 h agitation in PBS containing 0.6 mM sulfobetaine-16 (SB-16) (Sigma) and 0.14% Triton X-200 (Sigma). After washing the specimens in PBS for 5 min, the nerve segments were placed in a PBS solution containing SB-10 for another 7 h. The specimens were then rinsed in PBS before being transferred to the SB-16 and Triton X-200 solutions for 15 h. Following a final wash with distilled water, ANAs were stored at 4°C in PBS (pH 7.4) containing 100 g/mL penicillin and 100 g/mL streptomycin. Before implantation, both ends of the ANA were trimmed to create a tidy 10 mm graft. For ANA/EpoB fabrication, EpoB (Abcam; ab141271) was dissolved in 20 μL of polyethylene glycol-300 (PEG300; Sigma)/normal saline (30/70) and injected into the ANA from both ends before implantation.

2.3 | Histological evaluation of ANA

Transverse sections of ANA were stained with toluidine blue to confirm myelin and axon elimination, as described previously. In brief, the specimens were fixed overnight in 4% paraformaldehyde (PFA) in PBS and then dehydrated in an ascending ethanol concentration before being embedded in paraffin. The blocks were cut into 5-μm-thick cross-sections, deparaffinized with xylene, and rehydrated with a descending ethanol series. Finally, specimens were stained with 1% toluidine blue (Fluka) and mounted with Entellan for light microscopy analysis [36]. Additionally, to confirm cell elimination, 1-μm-thick cross-sections of ANA were stained with DAPI, as previously described [37]. Deparaffinized and rehydrated cross-sections were incubated in the dark for 15 min with a DAPI staining solution (200 μL). The slides were examined using a fluorescence microscope. Hematoxylin–eosin (H&E) staining was also performed as previously described [8].

2.4 | Surgical method

The same surgeon performed the surgeries under aseptic conditions. The rats were anesthetized with intraperitoneal injections of ketamine (80 mg/kg; Alfasan Pharmaceutical Co., Holland) and xylazine (10 mg/kg; Alfasan Pharmaceutical Co., Holland) before being placed in the prone position on a heating pad (37 ± 1°C). Afterward, the left sciatic nerve was exposed, a 10-mm-long sciatic nerve segment was removed proximal to the sciatic nerve trifurcation, and the gap was bridged with a 10 mm ANA with four epineural sutures (10-0 nylon, Ethicon). In the autograft group, 10 mm of the sciatic nerve was excised, reversed, and re-implanted with epineural sutures into the nerve gap. Finally, the muscles and skin were sutured (6-0 prolene; Ethicon), and the animals were allowed to recover from anesthesia. Rats in the sham-operated group were also subjected to surgical procedures but without nerve injuries. All operated animals received a once-daily dose of buprenorphine (0.05 mg/kg) subcutaneously for 3 days after surgery. To prevent autotomy, bitter nail polish was applied to the operated limb [38].

2.5 | Sciatic functional index (SFI)

The SFI was calculated preoperatively and every 4 weeks for the next 16 weeks to assess motor function recovery. Briefly, rats with black ink-painted hind limbs were allowed to leave footprints down a white sheet-covered corridor. Then, the distance between the third toe tip and the hind limb pads (paw length [PL]), the first and fifth toes (toe spread [TS]), and the second and fourth toes (intermediary toe spread [ITS]) were measured by a blind operator. The SFI was calculated as follows: $SFI = -38.3\ [(EPL-NPL)/NPL] + 109.5\ [(ETS-NTS)/NTS] + 13.3\ [(EIT-NIT)/NIT] - 8.8$, where E and N represent injured and uninjured paws, respectively [39].

2.6 | Hot plate test

Thermal paw withdrawal reflex latency (PWRL) was evaluated preoperatively, 4, 8, 12, and 16 weeks after surgery to determine sensory recovery. In brief, rats were restrained above the waist and placed on a hot plate (55 ± 1°C; PE34, IITC Life Sciences, USA) with their affected hind paw. PWRL was defined as the time elapsed between the hotplate touch and the PWRL emerging. All assays were carried out in triplicate at 2 min intervals, and averages were reported. We set the cut-off time to 12 s to avoid injury to the foot tissue [40].

2.7 | Electrophysiological evaluation

We measured the compound muscle action potential (CMAP) and motor nerve conduction velocity (NCV) under anesthesia in the 16th postoperative week (9). In brief, the animal was anesthetized with a ketamine (80 mg/kg) and xylazine (10 mg/kg) cocktail before being placed prone on a heating pad (37 ± 1°C). A bipolar hook electrode was placed 5 mm proximal to the graft site. The active recording needle electrode and the reference needle electrode were then inserted into the muscle belly and Achilles tendon, respectively. The ground electrodes were also placed in the animal's tail. The sciatic nerve was stimulated with supramaximal square-wave pulses of 0.2 ms duration and 0.5 ms intervals to produce the maximum CMAP response. The CMAP signal was captured at 10 kHz and then low-pass and high-pass filtered at 10 Hz and 1 kHz, respectively. Furthermore, the NCV was calculated by dividing the distance between the stimulating and recording electrodes by the CMAP latency. The normal CMAP and NCV were measured on the uninjured contralateral sciatic nerve [41]. CMAP measures muscle reinnervation quality, whereas NCV measures the maturity and remyelination of regenerated axons. By measuring these parameters, we hoped to compare the quality of nerve regeneration and target organ reinnervation among groups. Because electrophysiological measurement is an invasive method that requires anesthesia, we omitted the CMAP and NCV examination over time to avoid tissue injuries and the risk of death caused by anesthetics.

2.8 | Histomorphometry analysis

After conducting electrophysiological assessments, the animals were euthanized by carbon dioxide asphyxiation. Then, the regenerated sciatic nerves were harvested 3–5 mm distally from the implanted grafts. In brief, the nerve segments were fixed in 4% PFA, dehydrated in ascending concentrations of ethanol, and embedded in resin. Finally, the blocked specimens were cut into 1-μm-thick transverse sections and stained with 1% toluidine blue for light microscopy analysis (Carl Zeiss, Germany). Histomorphometric analysis was performed on a single sciatic nerve cross-section from each rat (a total of seven samples from each group). The sciatic nerve cross-sections were imaged at 400× magnification using a light microscope equipped with an Olympus DP72 camera. Ten overlapping photomicrographs were stitched together to cover the entire nerve cross-section in ImageJ (National Institutes of Health, Maryland). The total fiber number in the nerve was then estimated by manually counting axons in 10% of the nerve cross-section. For this purpose, a sampling frame grid was placed on each nerve cross-section image, and a blind observer counted myelinated axons within each sampling field (selected through systematic random sampling), as well as the upper and left borders. The diameters of the axon and fiber were both measured. From these measurements, the thickness of the myelin and the g-ratio were calculated using the formulas [(fiber diameter − axon diameter)/2] and axon diameter/fiber diameter. The uninjured contralateral limb's sciatic nerve was considered a healthy control [42].

2.9 | Gastrocnemius muscle mass ratio

The gastrocnemius muscle mass ratio was measured to determine nerve reinnervation and muscle atrophy. Following the electrophysiological evaluation, gastrocnemius muscles were harvested from the experimental and contralateral sides and weighed immediately. Then, the muscle mass ratio was calculated by dividing the muscle weight on the operated side (left) by the muscle weight on the contralateral side (right) [43].

2.10 | Real-time polymerase chain reaction (real-time PCR)

The mRNA levels of $p75^{NTR}$ as SC-related genes, as well as NGF and BDNF, were determined by real-time PCR 7 days after surgery. In brief, total RNA was extracted from sciatic nerve grafts using a Total RNA Extraction Kit (Promega, USA) according to the manufacturer's protocol. After quantifying RNA quality and yield using a Thermo Fisher Scientific Nanodrop ND-1000 spectrophotometer, 1 μg of total RNA was reverse transcribed into cDNAs in a final reaction volume of 20 μL using the Moloney Murine Leukemia Virus Reverse Transcriptase (M-MLV RT; Promega, USA). Finally, 1 μL of cDNA was amplified by the Corbett thermal cycler (Corbett Research, Australia) in the presence of forward and reverse primers (500 nM) and 2× Power SYBR Green Master Mix (Invitrogen) under the following conditions: pre-denaturation at 95°C for 5 min, 35 cycles

of denaturation at 94°C for 30 s, annealing at 57°C for 20 s, elongation at 72°C for 30 s, and final elongation at 72°C for 5 min. All assays were run in triplicate with the same samples, and the target gene expression was normalized with glyceraldehyde 3-phosphate dehydrogenase (GAPDH) as an internal control. The relative mRNA expression was calculated using the $2^{-\Delta\Delta Ct}$ method and normalized with GAPDH mRNA as an internal control. Table 1 shows the primer sequences that were obtained from a previous study [44, 45].

2.11 | Statistical analysis

Data are analyzed with SPSS Statistics 20.0 (SPSS Inc., Chicago, Illinois, USA). The Kolmogorov–Smirnoff test was applied to determine the data's normality. A one-way analysis of variance (ANOVA) was used for the comparison of multiple groups. To compare the two groups, a Tukey post hoc analysis was employed. $P < 0.05$ was considered statistically significant, and all data are presented as mean ± standard deviations.

3 | RESULTS

This study aimed to assess the regenerative effects of ANA loaded with EpoB for the reconstruction of the rat sciatic nerve gap. Autotomy necessitated euthanizing two animal from the ANA and ANA/EpoB (10 nM) groups using carbon dioxide asphyxiation. Other animals survived without visible neuroma or inflammation. In terms of measured parameters, there was no significant difference between the healthy control and sham surgery groups, as well as the ANA/vehicle and ANA groups. As a result, data from the healthy control and ANA/vehicle groups were excluded for simplicity.

3.1 | Characterization of ANA

The ANA appeared whitish and transparent under macroscopic examination. H&E staining (Figure 1a) and DAPI nuclear staining (Figure 1c) confirmed the elimination of axons, myelin, and cells from the ANA. However, the ECM and basement membrane were preserved in a wave-like pattern (Figure 1a). Toluidine blue staining also provides further evidence of myelin elimination from ANA (Figure 1e). Healthy nerves have intact axons and myelin sheaths (Figure 1b,f), with deep blue SCs nuclei (Figure 1d).

TABLE 1 Specific primer sequences for real-time PCR.

Primer	Sequence
NGF	F: 5′-ACA CTC TGA TCA CTG CGT TTT TG-3′ R: 5′-CCT TCT GGG ACA TTG CTA TCT GT-3′
BDNF	F: 5′-CCATAAGGACGCGGACTTGTAC-3′ R: 5′-AGACATGTTTGCGGCATCCAGG-3′
$p75^{NTR}$	F: 5′-CATCTCTGTGGACAGCCAGA-3′ R: 5′-CTCTACCTCCTCACGCTTGG-3′
GAPDH	F: 5′-TTCGCAAAACAAGTTCACCA-3′ R: 5′-TCGTTGTGGTTGTAAATGGAA-3′

3.2 | SFI

Motor recovery after sciatic nerve injury is assessed using SFI scores ranging from 0 (*normal function*) to −100 (*complete dysfunction*). Animals with normal motor function before surgery experienced severe leg paralysis in the fourth week after nerve injury, with SFI values approaching −100, except in the sham group (Figure 2). As can be seen in Figure 2, SFI scores improved at different rates in all nerve-deficient animals over time, indicating partial locomotor recovery and muscle reinnervation. However, the ANA/EpoB (0.1 nM) group showed significantly higher SFI restoration at the fourth, eighth, 12th, and 16th weeks post-surgery compared to the ANA, ANA/EpoB (1 nM), and ANA/EpoB (10 nM) groups (Figure 2; $P < 0.05$). When compared to the nerve autograft group, the ANA/EpoB (0.1 nM) group had significantly lower SFI recovery (Figure 2; $P < 0.05$). Furthermore, both the ANA and ANA/EpoB (1 nM) groups outperformed the ANA/EpoB (10 nM) group in SFI values across all measurement times (Figure 2; $P < 0.05$). However, no significant difference was found between the ANA and ANA/EpoB (1 nM) groups. Sham surgery did not affect the SFI score, so the data are not shown in Figure 2 for simplicity.

3.3 | Hot plate

Thermal PWRL assessed sensory function recovery before and post-surgery for 16 weeks. Four weeks post-surgery, PWRL reached 12 s (cut-off time) in all groups except the sham group, indicating severe sensory dysfunction (Figure 3). Afterward, animals with nerve grafts showed a gradual decrease in PWRL, indicating successful regeneration of axons and reinnervation of paw skin. However, PWRL in the ANA/EpoB (0.1 nM) group improved more than the ANA, ANA/EpoB (1 nM), and ANA/EpoB (10 nM) groups in the eighth, 12th, and 16th weeks after surgery (Figure 3; $P < 0.05$). Nonetheless, sensory function recovery in the ANA/EpoB (0.1 nM) group was lower than in the autograft group ($P < 0.01$). Furthermore, both the ANA and ANA/EpoB (1 nM) groups outperformed the ANA/EpoB (10 nM) group in PWRL restoration across the eighth, 12th, and 16th weeks ($P < 0.05$). At the same time points, the ANA/EpoB (1 nM) group

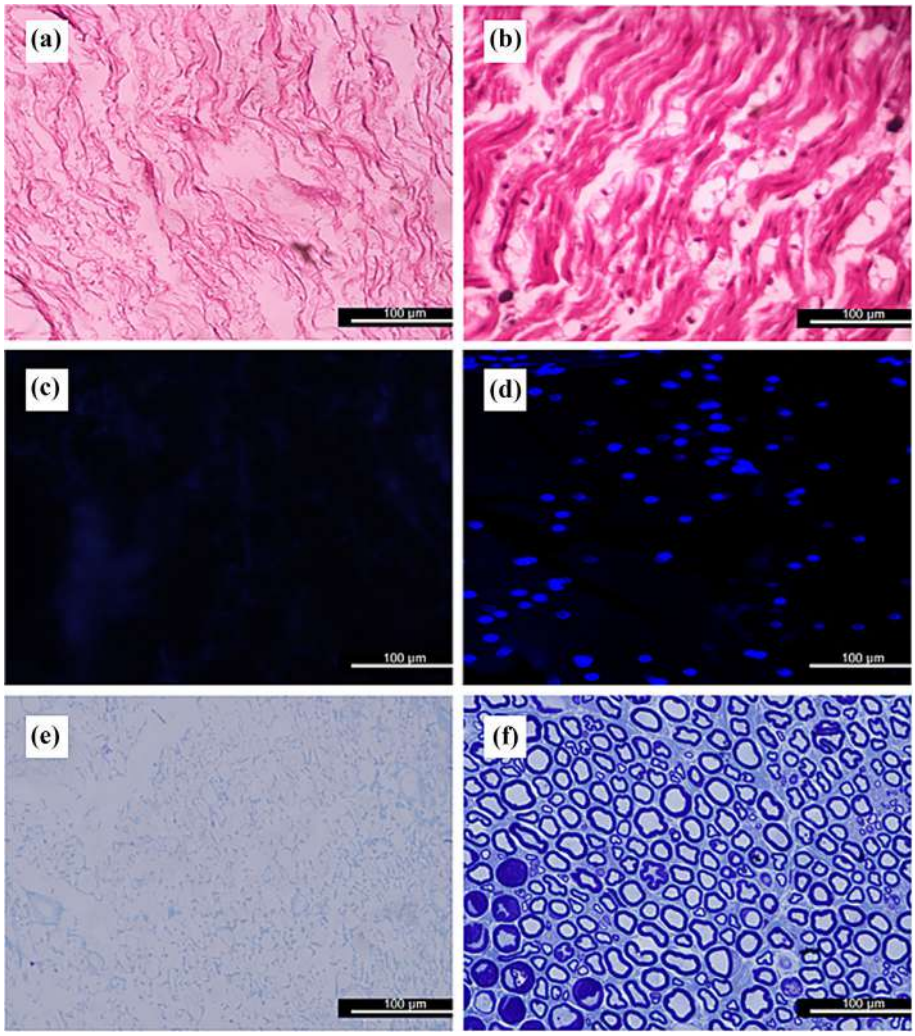

FIGURE 1 Histological assessment of the decellularized sciatic nerve allografts. Hematoxylin–eosin staining shows the morphology of a decellularized sciatic nerve allograft longitudinal section (a) and a fresh rat sciatic nerve longitudinal section (b). The Schwann cell nuclei were stained in deep blue, and the myelin sheaths were mesh-like with faint staining in fresh nerve. Axons and cell nuclei, on the other hand, were missing from the decellularized nerve. DAPI staining confirmed cell nucleus elimination from the decellularized nerve allograft (c) compared with the intact nerve (d). Toluidine blue staining also revealed the elimination of myelination sheaths from the decellularized nerve (e) compared to the intact nerve cross-section (f).

was significantly superior to the ANA group (Figure 3; $P < 0.05$). The sham surgery did not affect normal PWRL, so the data are not shown in Figure 3.

3.4 | Electrophysiological evaluation

Electrophysiological measurements at the 16th week postoperatively quantified CMAP amplitudes and NCV in injured limbs. The autograft group showed the most prominent CMAP amplitude recovery (Figure 4a) and NCV restoration (Figure 4b) compared to other grafted groups ($P < 0.05$). Similarly, the ANA/EpoB group (0.1 nM) showed superior CMAP amplitude and NCV compared to the ANA, ANA/EpoB (1 nM), and ANA/EpoB (10 nM) groups (Figure 4a,b; $P < 0.01$). On the other hand, the ANA and ANA/EpoB (1 nM) groups showed superiority in CMAP amplitude and NCV compared to the ANA (10 nM) group ($P < 0.05$), but there was no significant difference among them. The sham surgery did not affect normal CMAP amplitudes or NCV, so no data are shown.

3.5 | Histomorphometry analysis

Toluidine blue staining compared axon regeneration and remyelination among groups (Figure 5), while Table 2 provided a morphometric analysis of sciatic nerves. According to the result, ANA/EpoB groups (0.1 nM) had higher myelinated fiber count, diameter, and myelin thickness compared to other ANA-implanted groups (Table 2, $P < 0.05$). However, all of the mentioned parameters were significantly lower in the ANA/EpoB group (0.1 nM) than in the autograft group ($P < 0.05$). Furthermore, myelinated fiber count, fiber diameter, and myelin thickness were higher in both ANA and ANA/EpoB (1 nM) groups compared to the ANA/EpoB (10 nM) group ($P < 0.05$). However, no significant difference was found between the ANA and ANA/EpoB (1 nM) groups in morphometric parameters. In addition, grafted groups have a higher g-ratio, indicating reduced myelin sheath thickness and a lower NCV than healthy nerves. The g-ratio is defined as the inner-to-outer diameter ratio of a myelinated axon.

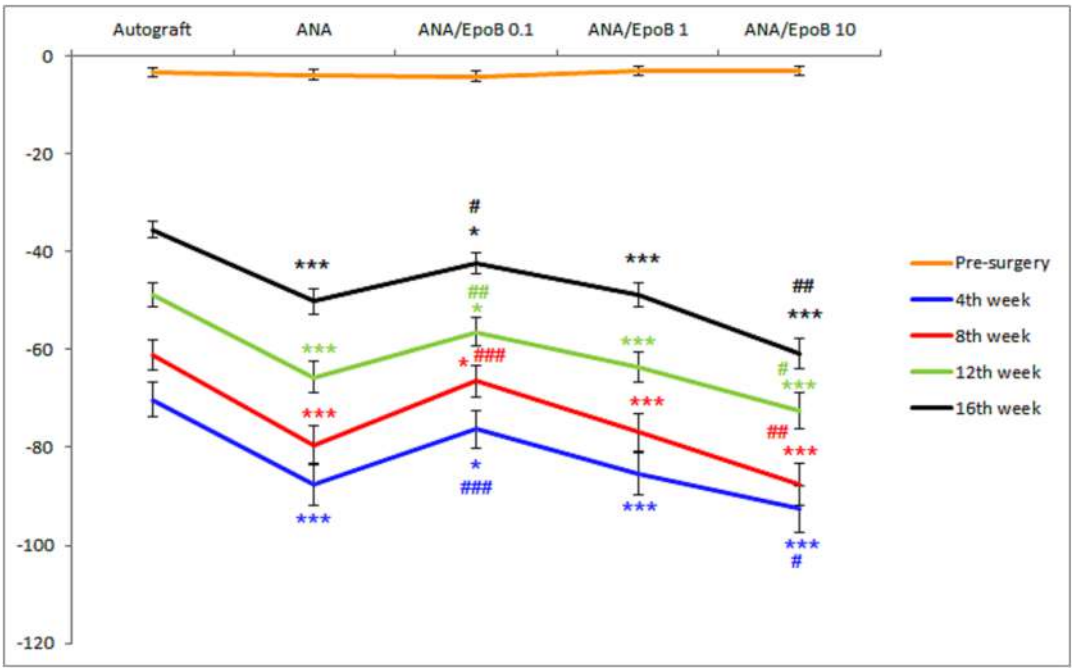

FIGURE 2 Assessment of motor function recovery using walkway track analysis and sciatic functional index (SFI) calculation. The SFI was assessed pre-surgery and every 4 weeks for the next 16 weeks. The data are presented as mean ± standard deviation (SD) ($n = 10$). $^{*}P < 0.05$, $^{**}P < 0.01$, and $^{***}P < 0.001$ for comparison with the nerve autograft group and $^{\#}P < 0.05$, $^{\#\#}P < 0.01$, and $^{\#\#\#}P < 0.001$ for comparison with the acellular nerve allograft (ANA) group.

FIGURE 3 Assessment of thermal pain threshold by measuring the thermal paw withdrawal reflex latency (PWRL). PWRL was pre-surgery and every 4 weeks for the next 16 weeks. The data were expressed as mean ± standard deviation (SD) ($n = 10$). $^{*}P < 0.05$, $^{**}P < 0.01$, and $^{***}P < 0.001$ for comparison with the nerve autograft group and $^{\#}P < 0.05$, $^{\#\#}P < 0.01$, and $^{\#\#\#}P < 0.001$ for comparison with the acellular nerve allograft (ANA) group.

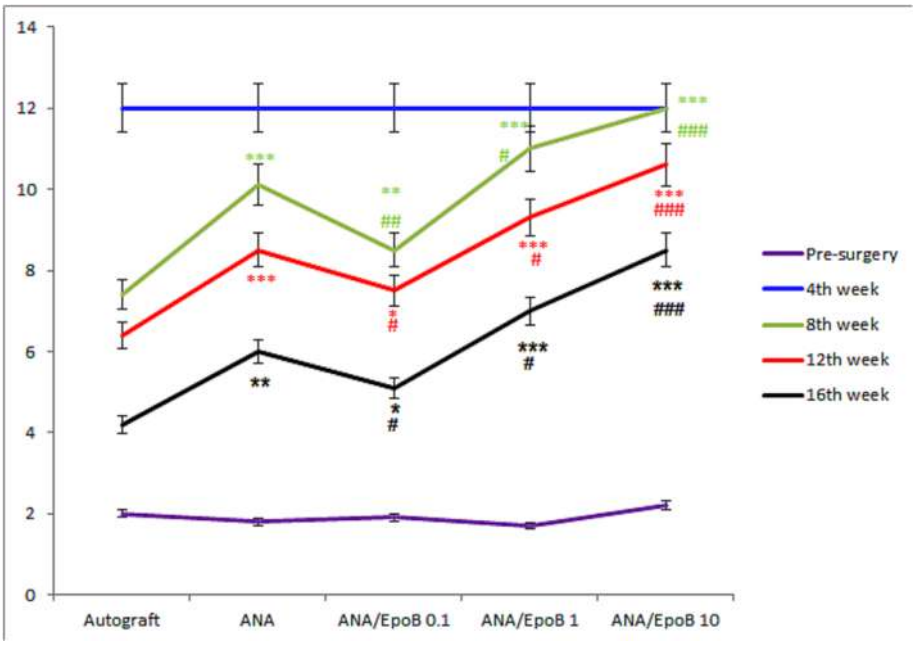

3.6 | Muscle mass ratio

The muscle mass ratio compares gastrocnemius muscle atrophy among groups. As illustrated in Figure 6, nerve-grafted animals showed muscle atrophy compared to the sham surgery group. The study found that the ANA/EpoB (0.1 nM) group had a higher muscle mass ratio compared to the ANA, ANA/EpoB (1 nM), and ANA/EpoB (10 nM) groups ($P < 0.01$). However, the ANA/EpoB (0.1 nM) group had a lower muscle mass ratio compared to the nerve autograft ($P < 0.01$). Furthermore, ANA and ANA/EpoB (1 nM) groups

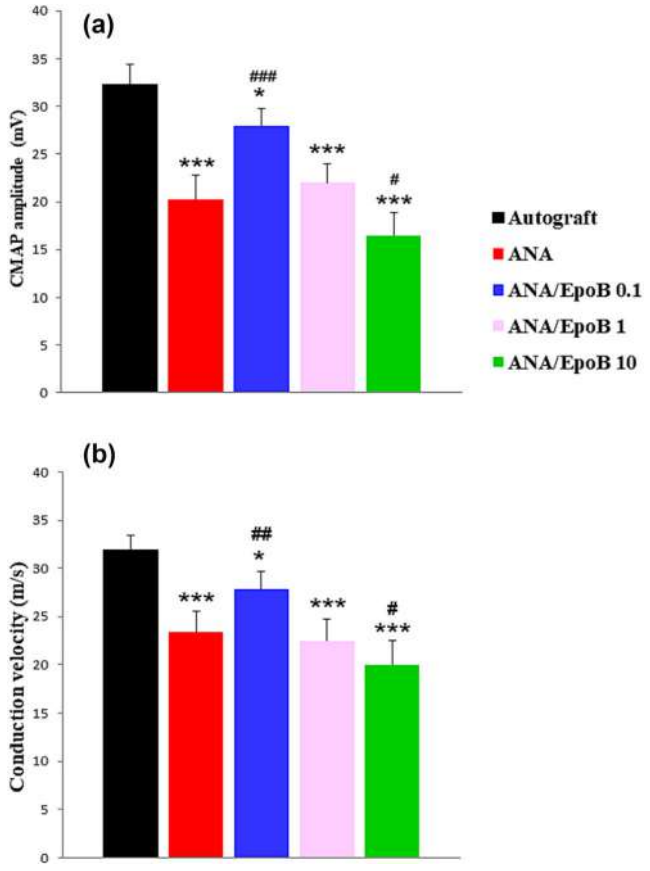

FIGURE 4 Electrophysiological assessments of the regenerated nerves. The compound muscle action potential (CMAP) and nerve conduction velocity (NCV) were assessed 16 weeks after surgery. After proximal stimulation, the CMAP amplitude (a) and NCV (b) were recorded at the gastrocnemius muscle of the operated side in each group. The data were expressed as mean ± standard deviation (SD) ($n = 10$). $^{*}P < 0.05$, $^{**}P < 0.01$, and $^{***}P < 0.001$ for comparison with the nerve autograft group and $^{\#}P < 0.05$, $^{\#\#}P < 0.01$, and $^{\#\#\#}P < 0.001$ for comparison with the acellular nerve allograft (ANA) group.

outperformed ANA/EpoB (10 nM) ($P < 0.05$). No significant difference was found between the ANA and ANA/EpoB (1 nM) groups.

3.7 | Real-time PCR

Real-time PCR assessed the mRNA levels of NGF, BDNF, and $p75^{NTR}$ in sciatic nerve allografts 7 days post-surgery. Figure 7 shows significantly increased mRNA levels of NGF, BDNF, and $p75^{NTR}$ in the ANA/EpoB (0.1 nM) group compared to the ANA, ANA/EpoB (1 nM), and ANA/EpoB (10 nM) groups ($P < 0.001$). Likewise, the ANA/EpoB (1 nM) group showed higher levels of NGF, BDNF, and $p75^{NTR}$ mRNA compared to the ANA/EpoB (10 nM) group ($P < 0.05$). Meanwhile, the autograft group had higher levels of NGF, BDNF, and $p75^{NTR}$ mRNA than the other groups ($P < 0.001$).

4 | DISCUSSION

Nerve autografting is currently the standard method in clinics for bridging long nerve gaps. However, the clinical application of nerve autographs has significant limitations [46]. As a result, various synthetic or biological scaffolds, such as decellularized nerves, have been proposed as alternatives to nerve autografts [47]. Nerve decellularization could be an effective method for producing a natural scaffold. This process involves removing cellular antigens from the nerve while preserving most of the ECM and internal nerve structure [48]. ECM provides a supportive substrate and environmental cues for cell differentiation and proliferation, which are necessary for tissue development and regeneration [49]. The availability of cadaveric nerve allografts also allows for the best choice of graft in terms of size and type of sensory, motor, or mixed nerve. Although ANA has regenerative properties comparable to autografts across short gaps, their efficacy declines across more extended defects [9]. Therefore, improving the regenerative properties of ANA is critical. We hypothesized that EpoB supplementation in ANA enhances scaffold regenerative properties by stabilizing microtubules and promoting axonal regeneration. As a result, the current study aimed to assess the regenerative potential of ANA-loaded EpoB in a rat model with sciatic nerve injury. Our research is the first to link the ANA-loaded EpoB with improving axonal regeneration. To assess the drug's dose-dependent effects, we supplemented ANA with three different concentrations of EpoB (0.1, 1, and 10 nM). Previous studies have shown that high concentrations of EpoB induce neurotoxicity, whereas low concentrations lead to neuroprotection [29]. We measured the expression of $p75^{NTR}$ (a specific SCs marker) and neurotrophic factors (NGF and BDNF) 7 days after nerve injury. Previous studies have shown that the peak of SC proliferation and neurotrophic factor expression occurs 7–14 days after nerve injury [50, 51]. According to our findings, the ANA/EpoB (0.1 nM) group had greater sensorimotor restoration than the ANA, ANA/EpoB (1 nM), and ANA/EpoB (10 nM) groups. ANA and ANA/EpoB (1 nM) groups showed similar mean SFI values, but the ANA/EpoB (1 nM) group experienced weaker PWRL recovery at the fourth, eighth, 12th, and 16th weeks post-surgery. As a result, the higher concentration of EpoB may have hampered sensory neuron regeneration. Furthermore, previous research has shown that cultured DRG neurons are more sensitive to the neurotoxic effects of high EpoB concentrations than motor neurons [29, 30]. If this is correct, the therapeutic window for EpoB may be reduced. The electrophysiological evaluation showed higher CMAP amplitude and NCV in the ANA/EpoB (0.1 nM) group compared to the ANA, ANA/EpoB (1 nM), and ANA/EpoB (10 nM) groups. NCV indicates motor nerve

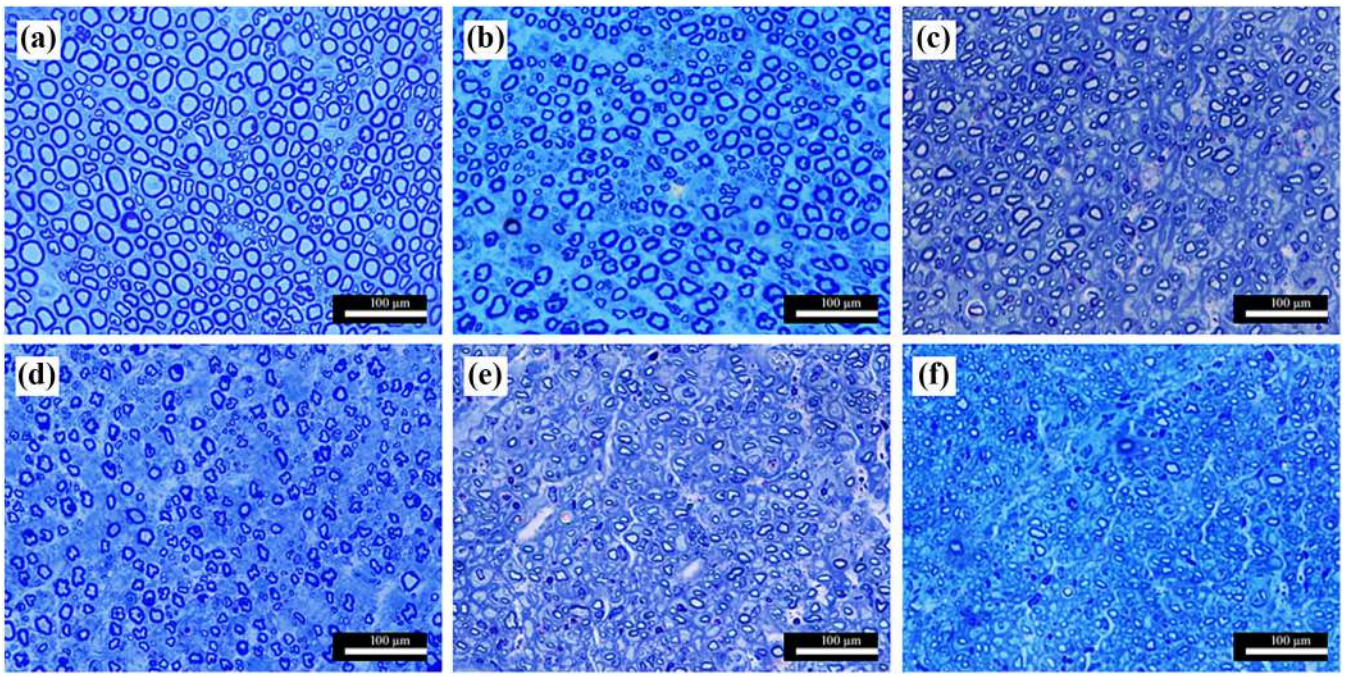

FIGURE 5 Toluidine blue staining of regenerated sciatic nerves in the 3–5 mm distal to the lesion site at the 16th postoperative week. (a) the sham group, (b) the autograft group, (c) the ANA group, (d) the ANA EpoB (0.1 nM) group, (e) the ANA EpoB (1 nM) group, and (f) the ANA EpoB (10 nM) group.

TABLE 2 Histomorphometry evaluation of myelinated axons in regenerated sciatic nerve cross-sections 16 weeks after surgery.

	Myelinated fiber count	Myelinated fiber diameter (μm)	Axon diameter (μm)	Myelin sheath thickness (μm)	g-Ratio
Sham	4437 ± 608***,###	6.1 ± 0.83**,###	3.9 ± 0.65*,###	1.1 ± 0.26***,###	0.64
Autograft	2336 ± 429	4.42 ± 0.73	3.2 ± 0.52	0.61 ± 0.17	0.72
ANA	1673 ± 290**	3.3 ± 0.75**	2.54 ± 0.48*	0.39 ± 0.11**	0.77
ANA/EpoB (0.1 nM)	2011 ± 316*,##	3.91 ± 0.63*,##	2.97 ± 0.60#	0.47 ± 0.14*,#	0.76
ANA/EpoB (1 nM)	1589 ± 228**	3.21 ± 0.69**	2.47 ± 0.48**	0.37 ± 0.12**	0.77
ANA/EpoB (10 nM)	1109 ± 268***,##	2.8 ± 0.8***,#	2.24 ± 0.51**	0.28 ± 0.09***,##	0.8

Note: Values are shown as mean ± SD ($n = 10$).
*$P < 0.05$ for comparison with the nerve autograft group.
**$P < 0.01$ for comparison with the nerve autograft group.
***$P < 0.001$ for comparison with the nerve autograft group.
#$P < 0.05$ for comparison with the acellular nerve allograft (ANA) group.
##$P < 0.01$ for comparison with the acellular nerve allograft (ANA) group.
###$P < 0.001$ for comparison with the acellular nerve allograft (ANA) group.

fiber maturation, while CMAP amplitude indicates axon number reinnervating the gastrocnemius muscle. Also, the sensory-motor findings that EpoB (0.1 nM) effectively enhances scaffold regenerative properties were supported by electrophysiological assays. However, CMAP amplitude recovers faster than SFI because the regenerated axons innervate larger motor units and muscle fibers. Moreover, gastrocnemius muscle atrophy in the ANA/EpoB (0.1 nM) group was significantly reduced compared to the ANA, ANA/EpoB (1 nM), and ANA/EpoB (10 nM) groups. Also, ANA/EpoB (0.1 nM) significantly elevated myelinated axon count, axon diameter, myelin thickness, and g-ratio compared to ANA, ANA/EpoB (1 nM), and ANA/EpoB (10 nM) groups. According to previous research, the ideal g-ratio is between 0.6 and 0.75. Therefore, regenerated fibers in rats grafted with ANA/EpoB (0.1 nM) have a more mature structure than ANA, ANA EpoB (1 nM), and ANA EpoB (10 nM). These results revealed the most successful nerve regeneration and muscle reinnervation in rats given ANA/EpoB (0.1 nM). The real-time PCR also revealed that the ANA/EpoB (0.1 nM) group had a higher mRNA level of the SCs marker $p75^{NTR}$ than the ANA, ANA/EpoB (1 nM), and ANA/EpoB (10 nM) groups. As a result, EpoB at a 0.1 nM concentration increased the total number of

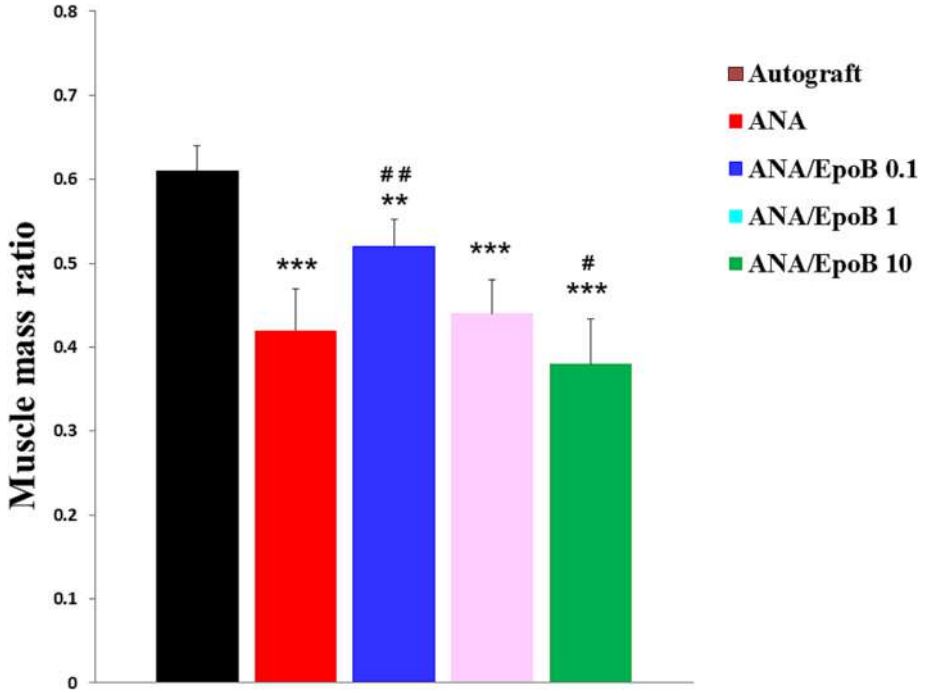

FIGURE 6 Gastrocnemius muscle atrophy assessment by measuring muscle mass ratio in experimental groups. The muscle mass ratio was determined by comparing the gastrocnemius muscle wet weight of the operated side to the non-operated side. The data are shown as mean ± SD ($n = 10$). $^{**}P < 0.01$ and $^{***}P < 0.001$ for comparison with the nerve autograft group and $^{\#}P < 0.05$ and $^{\#\#}P < 0.01$ for comparison with the acellular nerve allograft (ANA) group.

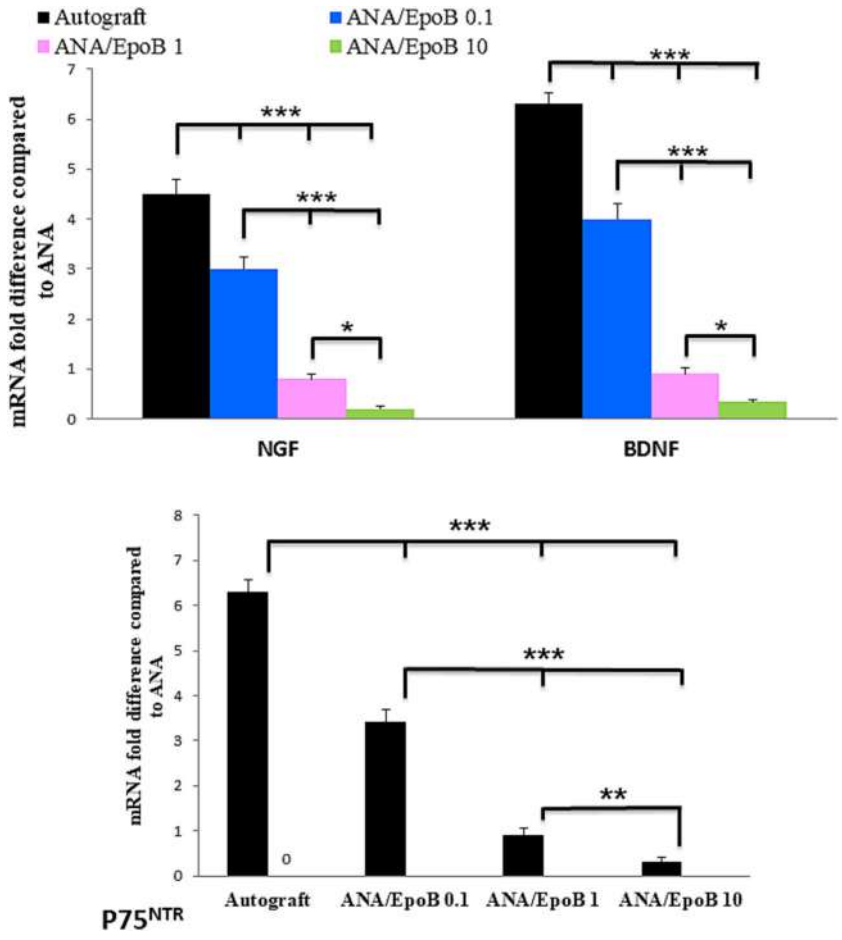

FIGURE 7 The real-time PCR assessment of NGF, BDNF, and $p75^{NTR}$ mRNAs in nerve grafts 7 days after surgery. Expression levels are represented relative to the respective mRNA level within the ANA group, which has been arbitrarily set to one. $^{*}P < 0.05$, $^{**}P < 0.01$, and $^{***}P < 0.001$.

SCs in the ANA 7 days after surgery. Although mature myelinating SCs do not express $p75^{NTR}$, $p75^{NTR}$ expression in SCs rises in response to nerve injury [52]. It is also highly expressed in non-myelinating SCs [53]. Following nerve grafting, SCs dedifferentiate and migrate progressively from both nerve stumps toward the implanted scaffold [54, 55]. Host-infiltrated SCs would improve axonal regeneration by producing neurotrophic factors, adhesion molecules, and axonal myelination [56]. Besides, the axonal growth cone interacts with ECM proteins such as fibronectin and laminin in the SC's external lamina [57–59]. Future research should consider SC migration, proliferation, and differentiation in ANA supplemented with EpoB. Additionally, the significant rise in the mRNA levels of NGF and BDNF in rats given ANA/EpoB (0.1 nM) may be related to the increase in the SC population in transplanted grafts. The NGF promotes sensory function recovery by enhancing sensory neuron sprouting and survival. BDNF, on the other hand, improves neuron survival, neurite outgrowth, and neuroplasticity after nerve injury. Furthermore, $p75^{NTR}$ expression promotes remyelination via a BDNF-dependent mechanism. Therefore, endogenous BDNF signaling disruption may impair myelination [60].

EpoB is an antineoplastic and microtubule-stabilizing macrolide that crosses the blood–brain barrier (BBB). Through glial-fibrotic scar inhibition, microtubule polymerization, and stabilization, EpoB promotes axon regeneration and sensorimotor recovery [25]. However, the effect of EpoB on peripheral nerves has received very little attention to date. In one of the few studies, Zhou et al. reported that EpoB promotes sensorimotor recovery and axon regeneration following sciatic nerve crush injury in adult male Sprague–Dawley rats. They treated the animals with 150 mg/mL EpoB intraperitoneally once daily for 7 days after surgery. They showed EpoB improves axonal regeneration by boosting SC migration, which is regulated by PI3K/Akt signaling-mediated autophagy. Treatment with EpoB also promotes axonal regeneration and remyelination, which improves sensorimotor recovery. Additionally, Zhou et al. investigated the effects of EpoB (0.25–4.0 nM) on the survival and migration of cultured SCs. Their findings revealed that treatment with 1 nM EpoB did not result in significant SC apoptosis while increasing SC migration. They concluded that EpoB can promote nerve regeneration by enhancing SC migration [28]. These findings are consistent with the findings of our study. However, in our study, therapeutic effects were only observed at a 0.1 nM EpoB concentration. In contrast, EpoB (10 nM) diminished SC marker expression, axon regeneration, and sensory-motor recovery. In an in vitro study, Chiorazzi et al. reported that EpoB (0.1, 0.5, and 5 nM) had a dose-dependent neurotoxic effect on cultured rat embryonic DRG neurons. According to their findings, a 24 h incubation with EpoB (0.1, 0.5, and 5 nM) reduced neurite outgrowth significantly ($P < 0.001$). DRG treated with EpoB at 0.1 and 0.5 nM showed recovery in neurite outgrowth after 48 h, while EpoB at 5 nM reduced neurite outgrowth ($P < 0.001$). At 50 nm concentrations, EpoB causes a severe decrease in neurite growth. Therefore, the lowest neurotoxic dose of EpoB was in the nanomolar range, which is comparable with our finding. In addition, in vivo evaluation shows EpoB (0.25 and 1.5 mg/kg/day) administration for 4 weeks causes dose-dependent neurotoxic effects and axonopathy in Fischer and Wistar rat sciatic nerves. EpoB significantly reduced NCV, increased axonal diameter, distal skin reinnervation, g-ratio, and prolonged PWRL (hypoalgesia) in the fourth week. EpoB increases tubulin polymerization in axons, but higher doses cause severe side effects, including weight loss and death in animals, despite being well tolerated at 0.25 mg/kg [29].

We concluded that EpoB's effects on mature, developing, healthy, and injured neurons may vary due to physiology and phenotype differences. The severity and type of injuries may impact its efficacy, requiring further investigation. In addition, EpoB, a cell division inhibitor, can cause adverse effects on tissues with dividing cells when administered systemically. For instance, EpoB administration may affect macrophage differentiation and proliferation, which are important for nerve regeneration. Furthermore, when EpoB is administered systemically, its cross-brain barrier potential may cause unwanted central nervous system effects. By loading EpoB into decellularized scaffolds, we exposed regenerating axons to EpoB locally, potentially minimizing systemic side effects. Based on our findings, ANA loaded with 0.1 nM EpoB successfully reconstructs a 10 mm sciatic nerve gap, promoting axonal regeneration and increasing SCs in grafts. Further research is needed to confirm the findings, as the study lacks a neuronal apoptosis study and direct assessment of SCs and macrophage proliferation and migration in response to EpoB treatment. Future research should explore EpoB's effects on Wallerian degeneration and macrophage behavior in injured nerves. Macrophages support axonal regeneration and axon sprouting.

5 | CONCLUSION

To our knowledge, this is the first time ANA loaded with low doses of EpoB has been used for reconstructing a peripheral nerve gap in a rat model. Results show that EpoB at low concentrations enhances ANA's regenerative properties, resulting in faster nerve regeneration and improved sensorimotor recovery compared to controls. Further research is needed to confirm these findings.

AUTHOR CONTRIBUTIONS

Arash Abdolmaleki and Zhikal Omar Khudhur designed the study, wrote the manuscript, and revised the manuscript. Shang Ziyad Abdulqadir contributed to writing and editing the manuscript. Abdullah Faqiyazdin Ahmed and Abdulrahman Aziz Rasoul contributed to analysis and interpretation of the data and take responsibility for the integrity of the data and the accuracy of the data analysis. Arash Abdolmaleki, Shukur Wasman Smail, and Mohammad B. Ghayour contributed to reviewing and editing the manuscript. All of the authors had full access to all of the data in the study.

ACKNOWLEDGMENTS

The work is supported by University of Mohaghegh Ardabili, Iran, and Tishk International University, Erbil, Kurdistan Region, Iraq (Grant 923). We thank them.

CONFLICT OF INTEREST STATEMENT

Authors have no conflicts of interest to declare.

ORCID

Arash Abdolmaleki https://orcid.org/0000-0003-2858-4098

REFERENCES

1. Lackington WA, Ryan AJ, O'Brien FJ. Advances in nerve guidance conduit-based therapeutics for peripheral nerve repair. *ACS Biomater Sci Eng*. 2017;3(7):1221-1235. doi:10.1021/acsbiomaterials.6b00500
2. Scheib J, Höke A. Advances in peripheral nerve regeneration. *Nat Rev Neurol*. 2013;9(12):668-676. doi:10.1038/nrneurol.2013.227
3. Siemionow M, Bozkurt M, Zor F. Regeneration and repair of peripheral nerves with different biomaterials: review. *Microsurgery*. 2010;30(7):574-588. doi:10.1002/micr.20799
4. Neubauer D, Graham JB, Muir D. Nerve grafts with various sensory and motor fiber compositions are equally effective for the repair of a mixed nerve defect. *Exp Neurol*. 2010;223(1):203-206. doi:10.1016/j.expneurol.2009.08.013
5. Mackinnon SE, Hudson AR. Clinical application of peripheral nerve transplantation. *Plast Reconstr Surg*. 1992;90(4):695-699. doi:10.1097/00006534-199210000-00024
6. Yu X, Bellamkonda RV. Tissue-engineered scaffolds are effective alternatives to autografts for bridging peripheral nerve gaps. *Tissue Eng*. 2003;9(3):421-430. doi:10.1089/107632703322066606
7. Struzyna LA, Harris JP, Katiyar KS, Chen HI, Cullen DK. Restoring nervous system structure and function using tissue engineered living scaffolds. *Neural Regen Res*. 2015;10(5):679-685. doi:10.4103/1673-5374.156943
8. Mohammad-Bagher G, Arash A, Morteza B-R, Naser M-S, Ali M. Synergistic effects of acetyl-l-carnitine and adipose-derived stromal cells on improving regenerative capacity of acellular nerve allograft in sciatic nerve defect. *J Pharmacol Exp Ther*. 2019;368(3):490-502. doi:10.1124/jpet.118.254540
9. Moore AM, Macewan M, Santosa KB, et al. Acellular nerve allografts in peripheral nerve regeneration: a comparative study. *Muscle Nerve*. 2011;44(2):221-234. doi:10.1002/mus.22033
10. Gulati AK, Cole G. Immunogenicity and regenerative potential of acellular nerve allografts to repair peripheral nerve in rats and rabbits. *Acta Neurochir*. 1994;126(2-4):158-164. doi:10.1007/BF01476427
11. Zheng C, Zhu Q, Liu X, et al. Improved peripheral nerve regeneration using acellular nerve allografts loaded with platelet-rich plasma. *Tissue Eng Part A*. 2014;20(23-24):3228-3240. doi:10.1089/ten.tea.2013.0729
12. Yu H, Peng J, Guo Q, et al. Improvement of peripheral nerve regeneration in acellular nerve grafts with local release of nerve growth factor. *Microsurgery*. 2009;29(4):330-336. doi:10.1002/micr.20635
13. Liu J, Li L, Zou Y, et al. Role of microtubule dynamics in Wallerian degeneration and nerve regeneration after peripheral nerve injury. *Neural Regen Res*. 2022;17(3):673-681. doi:10.4103/1673-5374.320997
14. Ruschel J, Bradke F. Systemic administration of epothilone D improves functional recovery of walking after rat spinal cord contusion injury. *Exp Neurol*. 2018;306:243-249. doi:10.1016/j.expneurol.2017.12.001
15. Petrášek J, Schwarzerová K. Actin and microtubule cytoskeleton interactions. *Curr Opin Plant Biol*. 2009;12(6):728-734. doi:10.1016/j.pbi.2009.09.010
16. Tanaka E, Ho T, Kirschner MW. The role of microtubule dynamics in growth cone motility and axonal growth. *J Cell Biol*. 1995;128(1):139-155. doi:10.1083/jcb.128.1.139
17. Gomez TM, Letourneau PC. Actin dynamics in growth cone motility and navigation. *J Neurochem*. 2014;129(2):221-234. doi:10.1111/jnc.12506
18. Bradke F, Fawcett JW, Spira ME. Assembly of a new growth cone after axotomy: the precursor to axon regeneration. *Nat Rev Neurosci*. 2012;13(3):183-193. doi:10.1038/nrn3176
19. Kalil K, Szebenyi G, Dent EW. Common mechanisms underlying growth cone guidance and axon branching. *J Neurobiol*. 2000;44(2):145-158. doi:10.1002/1097-4695(200008)44:2%3C145::AID-NEU5%3E3.0.CO;2-X
20. Dent EW, Gertler FB. Cytoskeletal dynamics and transport in growth cone motility and axon guidance. *Neuron*. 2003;40(2):209-227. doi:10.1016/S0896-6273(03)00633-0
21. Lowery LA, Vactor DV. The trip of the tip: understanding the growth cone machinery. *Nat Rev Mol Cell Biol*. 2009;10(5):332-343. doi:10.1038/nrm2679
22. Mahmoodi N, Ai J, Hassannejad Z, et al. Improving motor neuron-like cell differentiation of hEnSCs by the combination of epothilone B loaded PCL microspheres in optimized 3D collagen hydrogel. *Sci Rep*. 2021;11(1):21722. doi:10.1038/s41598-021-01071-2
23. Ruschel J, Hellal F, Flynn KC, et al. Systemic administration of epothilone B promotes axon regeneration after spinal cord injury. *Science*. 2015;348(6232):347-352. doi:10.1126/science.aaa2958
24. Yang Y, Zhang X, Ge H, et al. Epothilone B benefits nigrostriatal pathway recovery by promoting microtubule stabilization after intracerebral hemorrhage. *J Am Heart Assoc*. 2018;7(2):e007626. doi:10.1161/JAHA.117.007626
25. Kugler C, Thielscher C, Tambe BA, et al. Epothilones improve axonal growth and motor outcomes after stroke in the adult mammalian CNS. *Cell Rep Med*. 2020;1(9):100159. doi:10.1016/j.xcrm.2020.100159
26. Yu Z, Yang L, Yang Y, et al. Epothilone B benefits nigral dopaminergic neurons by attenuating microglia activation in the 6-hydroxydopamine lesion mouse model of Parkinson's disease. *Front Cell Neurosci*. 2018;12:324. doi:10.3389/fncel.2018.00324
27. Cartelli D, Casagrande F, Busceti CL, et al. Microtubule alterations occur early in experimental parkinsonism and the microtubule stabilizer epothilone D is neuroprotective. *Sci Rep*. 2013;3(1):1837. doi:10.1038/srep01837
28. Zhou J, Li S, Gao J, et al. Epothilone B facilitates peripheral nerve regeneration by promoting autophagy and migration in Schwann cells. *Front Cell Neurosci*. 2020;14:143. doi:10.3389/fncel.2020.00143

29. Chiorazzi A, Nicolini G, Canta A, et al. Experimental epothilone B neurotoxicity: results of in vitro and in vivo studies. *Neurobiol Dis*. 2009;35(2):270-277. doi:10.1016/j.nbd.2009.05.006
30. Jang E-H, Sim A, Im S-K, Hur E-M. Effects of microtubule stabilization by epothilone B depend on the type and age of neurons. *Neural Plast*. 2016;2016:5056418. doi:10.1155/2016/5056418
31. Ciccozzi M, Menga R, Ricci G, et al. Critical review of sham surgery clinical trials: confounding factors analysis. *Ann Med Surg*. 2016;12:21-26. doi:10.1016/j.amsu.2016.10.007
32. Wasman Smail S, Ziyad Abdulqadir S, Omar Khudhur Z, et al. IL-33 promotes sciatic nerve regeneration in mice by modulating macrophage polarization. *Int Immunopharmacol*. 2023;123:110711. doi:10.1016/j.intimp.2023.110711
33. Hu Y, Wu Y, Gou Z, et al. 3D-engineering of cellularized conduits for peripheral nerve regeneration. *Sci Rep*. 2016;6(1):32184. doi:10.1038/srep32184
34. Kim J-H, Choi Y-J, Park H-I, Ahn K-M. The effect of FK506 (tacrolimus) loaded with collagen membrane and fibrin glue on promotion of nerve regeneration in a rat sciatic nerve traction injury model. *Maxillofacial Plastic Reconstr Surg*. 2022;44(1):14. doi:10.1186/s40902-022-00339-5
35. Hudson TW, Liu SY, Schmidt CE. Engineering an improved acellular nerve graft via optimized chemical processing. *Tissue Eng*. 2004;10(9–10):1346-1358. doi:10.1089/ten.2004.10.1346
36. Raimondo S, Fornaro M, Di Scipio F, Ronchi G, Giacobini-Robecchi MG, Geuna S. Methods and protocols in peripheral nerve regeneration experimental research: part II—morphological techniques. *Int Rev Neurobiol*. 2009;87:81-103. doi:10.1016/S0074-7742(09)87005-0
37. Kerrison P, Steinke M. DAPI staining protocol. 2010.
38. Bernal J, Baldwin M, Gleason T, Kuhlman S, Moore G, Talcott M. Guidelines for rodent survival surgery. *J Invest Surg*. 2009;22(6):445-451. doi:10.3109/08941930903396412
39. Sarikcioglu L, Demirel B, Utuk A. Walking track analysis: an assessment method for functional recovery after sciatic nerve injury in the rat. *Folia Morphol*. 2009;68(1):1-7.
40. Hargreaves K, Dubner R, Brown F, Flores C, Joris J. A new and sensitive method for measuring thermal nociception in cutaneous hyperalgesia. *Pain*. 1988;32(1):77-88. doi:10.1016/0304-3959(88)90026-7
41. Schulz A, Walther C, Morrison H, Bauer R. In vivo electrophysiological measurements on mouse sciatic nerves. *J Vis Exp*. 2014;(86):e51181. doi:10.3791/51181-v
42. Scipio FD, Raimondo S, Tos P, Geuna S. A simple protocol for paraffin-embedded myelin sheath staining with osmium tetroxide for light microscope observation. *Microsc Res Tech*. 2008;71(7):497-502. doi:10.1002/jemt.20577
43. Varejão AS, Melo-Pinto P, Meek MF, Filipe VM, Bulas-Cruz J. Methods for the experimental functional assessment of rat sciatic nerve regeneration. *Neurol Res*. 2004;26(2):186-194. doi:10.1179/016164104225013833
44. Marrocco F, Delli Carpini M, Garofalo S, et al. Short-chain fatty acids promote the effect of environmental signals on the gut microbiome and metabolome in mice. *Commun Biol*. 2022;5(1):517. doi:10.1038/s42003-022-03468-9
45. Piovesana R, Faroni A, Taggi M, et al. Muscarinic receptors modulate Nerve Growth Factor production in rat Schwann-like adipose-derived stem cells and in Schwann cells. *Sci Rep*. 2020;10(1):7159. doi:10.1038/s41598-020-63645-w
46. Geissler J, Stevanovic M. Management of large peripheral nerve defects with autografting. *Injury*. 2019;50:S64-S67. doi:10.1016/j.injury.2019.10.051
47. Gu X, Ding F, Williams DF. Neural tissue engineering options for peripheral nerve regeneration. *Biomaterials*. 2014;35(24):6143-6156. doi:10.1016/j.biomaterials.2014.04.064
48. Fu R-H, Wang Y-C, Liu S-P, et al. Decellularization and recellularization technologies in tissue engineering. *Cell Transplant*. 2014;23(4-5):621-630. doi:10.3727/096368914X678382
49. Lin MY, Manzano G, Gupta R. Nerve allografts and conduits in peripheral nerve repair. *Hand Clin*. 2013;29(3):331-348. doi:10.1016/j.hcl.2013.04.003
50. Önger ME, Delibaş B, Türkmen AP, Erener E, Altunkaynak BZ, Kaplan S. The role of growth factors in nerve regeneration. *Drug Discov Ther*. 2016;10(6):285-291. doi:10.5582/ddt.2016.01058
51. Li R, Li D-H, Zhang H-Y, Wang J, Li X-K, Xiao J. Growth factors-based therapeutic strategies and their underlying signaling mechanisms for peripheral nerve regeneration. *Acta Pharmacol Sin*. 2020;41(10):1289-1300. doi:10.1038/s41401-019-0338-1
52. Tomita K, Kubo T, Matsuda K, et al. The neurotrophin receptor p75NTR in Schwann cells is implicated in remyelination and motor recovery after peripheral nerve injury. *Glia*. 2007;55(11):1199-1208. doi:10.1002/glia.20533
53. Assinck P, Sparling JS, Dworski S, et al. Transplantation of skin precursor-derived Schwann cells yields better locomotor outcomes and reduces bladder pathology in rats with chronic spinal cord injury. *Stem Cell Rep*. 2020;15(1):140-155. doi:10.1016/j.stemcr.2020.05.017
54. Zhang C, Zhang P, Wang Y, Yu K, Kou Y, Jiang B. Early spatiotemporal progress of myelinated nerve fiber regenerating through biological chitin conduit after injury. *Artif Cells Blood Subst Biotechnol*. 2010;38(2):103-108. doi:10.3109/10731191003634836
55. Min Q, Parkinson DB, Dun XP. Migrating Schwann cells direct axon regeneration within the peripheral nerve bridge. *Glia*. 2021;69(2):235-254. doi:10.1002/glia.23892
56. Saheb-al-Zamani M, Yan Y, Farber SJ, et al. Limited regeneration in long acellular nerve allografts is associated with increased Schwann cell senescence. *Exp Neurol*. 2013;247:165-177. doi:10.1016/j.expneurol.2013.04.011
57. Namgung U. The role of Schwann cell-axon interaction in peripheral nerve regeneration. *Cell Tissue Org*. 2015;200(1):6-12. doi:10.1159/000370324
58. Lefcort F, Venstrom K, McDonald JA, Reichardt LF. Regulation of expression of fibronectin and its receptor, alpha 5 beta 1, during development and regeneration of peripheral nerve. *Development*. 1992;116(3):767-782. doi:10.1242/dev.116.3.767
59. Gao X, Wang Y, Chen J, Peng J. The role of peripheral nerve ECM components in the tissue engineering nerve construction. *Rev Neurosci*. 2013;24(4):443-453. doi:10.1515/revneuro-2013-0022
60. McGregor CE, English AW. The role of BDNF in peripheral nerve regeneration: activity-dependent treatments and Val66-Met. *Front Cell Neurosci*. 2019;12:522. doi:10.3389/fncel.2018.00522

How to cite this article: Omar Khudhur Z, Ziyad Abdulqadir S, Faqiyazdin Ahmed Mzury A, et al. Epothilone B loaded in acellular nerve allograft enhanced sciatic nerve regeneration in rats. *Fundam Clin Pharmacol*. 2024;38(2):307-319. doi:10.1111/fcp.12961